MONITORING SUMMER SOLAR ULTRAVIOLET (UV) RADIATION ON THE GROUND LEVEL OVER ARDABIL-SAREIN, NW IRAN

R. Jahdi[1 *], M. Arabi[2, 3]

[1]University of Mohaghegh Ardabili, Faculty of Agriculture and Natural Resources, Ardabil, I.R. Iran - roghayeh.jahdi@uma.ac.ir
[2]Shahid Rajaee Teacher Training University, Tehran, I.R. Iran- Mahdi.a@sru.ac.ir
[3]University of Southern Queensland (USQ), Toowoomba, Queensland, Australia

Commission IV, WG IV/3

KEY WORDS: Earth's Surface, Solar UV Radiation, Temporal, Geographical Location, Solar Zenith Angle.

ABSTRACT:

The UV radiation level at the Earth's surface is generally affected by several factors such as time, geographic location, and climate. The first observations of solar UV radiation ever made in NW Iran, obtained in June 2019 are reported in this work. The analysis of hourly values of UV irradiances measured in the study area reveals significant diurnal variation during daylight hours, with lower values in the morning and afternoon and higher around noon. Mean hourly UV (A+B) ranged from 2755 to 10434 μW/cm^2 with an average value being about 7960 μW/cm^2. Mean hourly UV (C) ranged from 40 to 91 μW/cm^2 with an average value being about 76 μW/cm^2. The results of a short but intense measurement campaign in Ardabil-Sarein indicate the trends for geographical latitude, longitude, and altitude from surface UV measurements. The UV intensity is associated with geographical longitude (r^2= 0.15 for UV (A+B); r^2= 0.13 for UV (C)). Furthermore, UV intensity varies with the local latitude in the study area. There is a strong linear relationship between average UV and altitude and a trend of rising UV with increasing altitude is obtained. A decrease in UV radiation with increasing solar zenith (°) was observed. However, the correlation between UV radiation and solar azimuth (°) was not significant. Understanding the factors influencing near-surface UV radiation through systematic ground-based UV will help determine whether long-term changes occur as a result of changes in cloud cover or climate change, and how specific it means to identifying the causes.

1. INTRODUCTION

Solar ultraviolet (UV) radiation plays an important role in a variety of photochemical and photobiological processes at or near the earth's surface (Madronich et al., 2018). Radiation in particular is crucial for the energy balance of the earth-atmosphere system (Kadad et al., 2022). However, there is global concern about the permanence of standard surface UV levels and the preservation of the ozone layer in the atmosphere of the earth. The potential health hazard from an increase in UV radiation can motivate the increase in UV observations (Porfirio et al., 2012). UV radiation plays an important role in solar energy applications and global climate change (Wild et al., 2005), for example, UV radiation directly affects the photosynthetic uptake of atmospheric carbon dioxide, ecosystem stability, and global biogeochemical cycles (Thomas et al., 2012). UV radiation can also cause direct and immediate damage to virtually all living organisms (sunburn, skin cancer, and cataracts) (Bilbao et al., 2011).

Although UV radiation has gradually become one of the most important research topics in atmospheric science, measuring sites for UV radiation are scarce throughout Iran due to the high cost of instrumentation. Studies on UV radiation in Iran are few and long-term spectral measurements of UV radiation are scarce in most parts of the country. Based on a survey in different cities in Iran (Bouzarjomehri and Tsapaki, 2012; Vatani et al. 2013; Babaee et al., 2016; Akhlaghi et al., 2018), the natural radiation dose rate is above the normal range, which indicates the need to regularly review, monitor and report the annual effective dose of natural radiation (Shahbazi-Gahrouei et al., 2013). Most of the northern and northwestern provinces of Iran have a high risk of esophageal cancer. Also, the central and western provinces are at medium risk and the southern regions are at low risk. Located in northwestern Iran, Ardabil has the highest incidence of esophageal cancer in Iran (Kolahdoozan et al., 2010; Khodadost et al., 2016). Radiometric analysis in the UV band is basis to create public policies related to the society health and well-being. In Ardabil province, in particular, it is important to increase the population awareness about the harmful effects of UV radiation, as this region has high levels of solar radiation all year round. Parts of the population are employed in tourism, agriculture, and service sectors and are likely to be directly exposed.

2. MATERIAL AND METHODS

2.1. General Description of the Study Area

The hourly radiometric data used in this analysis was collected in June 2019 at an urban site between the municipalities of Ardabil and Sarein in Ardabil province in northwestern Iran, an area 70 km inland from the western Caspian coast (Figure 1). These communities are located in the western province of Ardabil, in areas leading

* Corresponding author

to the Sabalan mountain range (4000 m; 3816 N, 4750 E). The study area was considered as a strip between 38°00′ to 38°22′ N latitude (length approximately 103 km) and 48°00′ to 48°20′ E longitude (width approximately 5 km) and thus covers the entire geographical area of approximately 182 km^2. Sarein is located in the western part of Ardabil, which is a pristine nature away from the hustle and bustle of crowded cities and can develop into one of the main tourist centers due to environmental and natural features as well as cultural and human attractions. The tourist town of Sarein is attractive to tourists in summer as it has various spas, most of which have medicinal purposes, and also because of the unique climate that has increased the number of tourists (Hooshyar and Barugh, 2014). The study area exhibits a wide variety of landscapes, including high mountains, plateaux, valleys and plains, which determine different climate types. The climate of the areas is mainly characterized by low rainfall with irregular distribution, extreme daily and annual temperatures, low humidity and high wind speeds. According to Köppen's climate classification, Ardabil and Sarein have semiarid and and Mediterranean climates, respectively (Tavoosi and Delara, 2010).

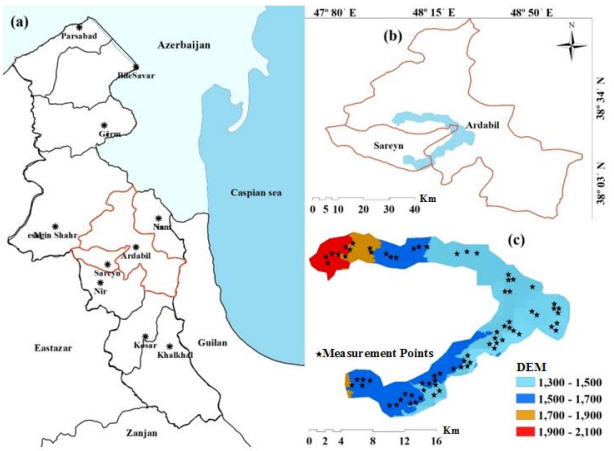

Figure 1. Maps of Ardabil Province, NW Iran, showing the location of the two Ardabil and Sarein municipalities (a); geographical locations of the study area in the two municipalities (b); and spatial distribution of UV (A+B) and UV (C) solar irradiances measurement points in the study area (c).

In the study area, four land use classes were established agriculture (60%), rangeland (32.5%), human-induced land use (7%), and water (0.5%). Major production in land under cultivation including irrigated (32%) and rain-fed (68%) are cereals (wheat, barley, chickpea, and lentils), industrial crops (cotton, oilseeds), vegetables (potato), fruits (apples, black cherry, peach, pears, cherry, and grapes), dry fruits (walnut) and other (alfalfa). Vegetation in the study area mainly includes lower vegetation and rangelands.

2.2. Measurement

The solar radiation that reaches the earth's surface varies in time: between day and night and also between the seasons due to the earth's rotation and the earth's orbit, respectively. At a specific time, it changes in space due to the changes in the obliquity of the sun's rays with longitude and latitude. Regardless of the clouds effects and other atmospheric parameters, the solar radiation received at a specific place and time according to the sun position and the earth. Because of this, time and sun-earth geometry play a critical role in the amount of solar radiation received at the earth's surface (Wald, 2018). Therefore, the main objective of this study is to introduce linear statistical models to estimate hourly UV radiation by examining the relationship between UV radiation and latitude, longitude and altitude, and altitude and azimuth of the sun based on measurements at 73 measurement points in the Study area in June 2019. Figure 1 shows the spatial distribution of the measuring points in the study area. This work also describes UV measurements made over several urban environmental surfaces: (vegetation, water, concrete, asphalt, soil).

UV (A+B) was measured with a handheld UVA/B light meter 850009 (Scottsdale, Arizona, USA) with a spectral sensitivity of 280 to 400 nm, covering spectral ranges of UVB and UVA. UV(C) measurements on a horizontal surface were made using a handheld UVC light meter 850010 (Scottsdale, Arizona, USA) with a spectral sensitivity of 220 to 275 nm. The UV radiometers used were calibrated by the manufacturer before the start of the measurement. The estimation of the relative error of the radiometers was less than 5% according to the manufacturer's expectation (see https://www.sperdirect.com/). These handy detectors are used to record time profiles of radiation over a wide range of time periods. During the investigation in the strip selected as the investigation area, measurements were carried out continuously and instantaneous values in irradiance units (W/cm^2) were recorded every 5 minutes; Hourly values were derived from the minute values by integration. UV (A+B) and UV (C) radiation were measured from different surfaces, such as 1) grass (lawn, meadow, and straw), 2) cultivated land (wheat, barley, potato, alfalfa, and spring vegetables (beans), 3) soil (arable soil, dirt road, hand soil) and water, as well as artificial surfaces, for example, asphalt and concrete. Visibility was very good overall during the measurement period (June 2019).

Linear regression is applied to assess the strength and direction of correlation coefficients. The selected independent variables of latitude, longitude, altitude, solar zenith, and azimuth angles are compared for their ability to show the observed variation in UV irradiance by calculation of the coefficients of determination (r^2).

3. RESULTS

3.1. Hourly variability of the UV irradiance

Solar UV radiation at the surface varies with atmospheric transmittance throughout the day independent of location. The hourly variability of the radiation for the measurement period is due to the components of atmospher under clear skies, as shown by the diurnal cycle of UV (A + B) and UV (C) (Figure 2a). The UV(A+B) profile was completely similar to that of UV(C), with the hours of the occurrence of the extremes (maximums and minima) coinciding; the increase (decrease) in UV (A + B) implies an increase (decrease) in UV (C). The highest UV values are reached in the midday hours. The maximum values for UV (A+B) and UV(C) irradiance were 11200 and 103 W/cm^2, respectively. Lower values of UV irradiance were 1950 and 23 W/cm^2 for UV (A+B) and UV(C) respectively). As can be seen in Figure 2a, UV(A+B) and UV(C) radiation increase with sun altitude and reach their maximum value between 12:00 and 13:00. It then decreases as the altitude of the sun decreases.

The data peaked around midday and shows moderate daily symmetry.

According to the results, the UV (A+B) and UV(C) irradiances increased progressively from 8.00 a.m. to mid-day then declined. They are lesser in the early hours of the morning and late afternoon and the maximum is between 12.00 and 13.00 (solar time). These findings are similar to the previous studies (Martinez-Lozano et al. 1996; Balasaraswathy et al. 2002; Bouzarjomehri and Tsapaki, 2012; Babaee et al., 2016; Pashiardis et al., 2017). According to the studies, outside the tropics, the highest levels occur when the sun is at its maximum elevation, at around midday (solar noon) during the summer months.

According to the results, UV(A+B) and UV(C) irradiance gradually increased from 8:00 a.m. to 12:00 p.m. and then decreased. They are lower in the early morning and late afternoon and the maximum is between 12:00 and 1:00 p.m. (solar time). These results are similar to previous studies (Martinez-Lozano et al. 1996; Balasaraswathy et al. 2002; Bouzarjomehri and Tsapaki, 2012; Babaee et al., 2016; Pashiardis et al., 2017). According to the studies, outside the tropics, the highest values occur when the sun is at its highest around noon (solar noon) in the summer months.

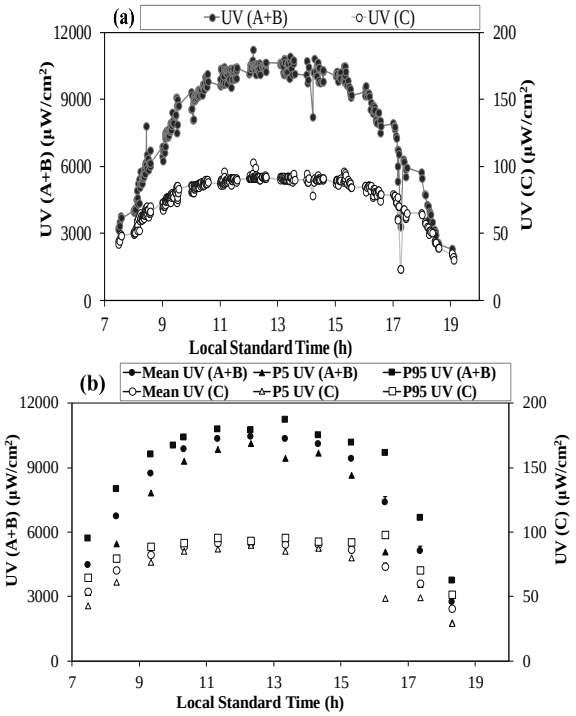

Figure 2. Daily patterns of UV (A+B) and UV (C) solar irradiances (a), under clear sky conditions: for the period (June 2019). Hourly mean, and percentiles P5 and P95 of UV (A+B) and UV (C) solar irradiances (b).

Hour	*N*	*M*	*SD*	*SE*	*Md*	*Mn*	*Mx*	*Q1*	*Q3*	*Q3- Q1*	*CV*	*P5*	*P95*
8	27	4441.59	765.8	147.4	4340	3160	5760	3960	5210	1250	17.2	3178	5705.16
9	55	6721.27	772.4	104.2	6700	5440	7920	6055	7480	1425	11.5	5446.8	7995.74
10	41	8724.15	539.1	84.19	8930	7500	9430	8270	9140	870	6.18	7834.7	9613.59
11	48	9842.71	342	49.36	9745	9180	10420	9590	10142.5	552.5	3.47	9278.5	10406.9
12	48	10307.9	283.9	40.97	10365	9500	11200	10182.5	10462.5	280	2.75	9839.6	10776.3
13	36	10434.2	192.3	32.06	10455	10090	10820	10327.5	10590	262.5	1.84	10117	10751.5
14	27	10321.5	539.3	103.8	10520	8180	10920	10115	10660	545	5.23	9431.6	11211.3
15	34	10094.7	251.5	43.13	10075	9710	10630	9905	10237.5	332.5	2.49	9679.8	10509.6
16	27	9394.07	461.9	88.88	9320	8370	10460	9155	10360	1205	4.92	8632	10156.1
17	29	7377.93	1391	258.4	7800	3270	8700	7240	10360	3120	18.9	5082.3	9673.54
18	15	5110	943.2	243.5	5470	3640	6290	4225	10360	6135	18.5	3553.7	6666.26
19	12	2755	585.1	168.9	2755	1950	3820	2302.5	10367.5	8065	21.2	1789.5	3720.48

Table 1. Hourly UV (A+B) solar irradiance (µW/cm^2) recorded in June 2019.

Hour	*N*	*M*	*SD*	*SE*	*Md*	*Mn*	*Mx*	*Q1*	*Q3*	*Q3- Q1*	*CV*	*P5*	*P95*
8	27	53.9	6.6	1.3	52	42	65	49.5	60.0	10.5	12.2	43.1	64.8
9	55	70.1	5.5	0.7	70	61	79	65.0	75.0	10	7.8	61.1	79.2
10	41	82.4	3.6	0.6	83	73	87	80.0	85.0	5	4.4	76.5	88.3
11	48	88.3	2.0	0.3	88	85	96	87.0	90.0	3	2.2	85.1	91.6
12	48	91.2	2.5	0.4	91	86	103	91.0	91.0	0	2.7	87.1	95.4
13	36	91.3	0.9	0.2	92	90	93	90.0	92.0	2	1.0	89.8	92.9
14	27	90.4	3.0	0.6	91	78	94	89.5	92.0	2.5	3.4	85.4	95.4
15	34	90.1	1.6	0.3	90	86	96	90.0	91.0	1	1.8	87.4	92.8
16	27	86.1	3.7	0.7	85	77	95	84.0	88.0	4	4.2	80.1	92.1
17	29	73.0	18.6	2.8	78	23	83	73.0	80.0	7	25.5	48.3	97.6
18	15	59.8	6.4	1.6	61	49	68	54.5	65.0	10.5	10.7	49.3	70.3
19	12	40.3	6.7	1.9	41	30	51	34.8	43.3	8.5	16.6	29.2	51.3

Table 2. Hourly UV (C) solar irradiance (µW/cm^2) recorded in June 2019.

This contribution has been peer-reviewed. The double-blind peer-review was conducted on the basis of the full paper.
https://doi.org/10.5194/isprs-annals-X-4-W1-2022-327-2023 | © Author(s) 2023. CC BY 4.0 License.

We analysed the statistical indices of hourly UV(A+B) and UV(C) values on a horizontal plane, which were arithmetic mean (M), the standard deviation (SD), the standard error (SE), the median (Md), the minimum value (Mn), the maximum value (Mx), the first (Q1) and the third (Q3) quartile, the interquartile range, the coefficient of variation (CV = 100SD/M), and the 5th (P5) and 95th (P95) percentile. The values of the indices are presented in Tables 1 and 2, where N is the number of values throughout. Figure 2b shows mean hourly values for both irradiances along with their corresponding P5, P95 and standard errors. In these tables, the hour parameter shows the local standard time (LST) centered on the corresponding values, for instance hour = 8 shows hourly values between 7:30 and 8:30. The summary of the tables is as follows:

1. The variation between the minimum value (Mn) and the P5 percentile is not large for both UV (A+B) and UV (C). This difference is more pronounced in the afternoon (14-17). The result demonstrated that the minimum values are more representative for the UV irradiance levels in the study area. The relatively high values of the minimum values can result from clear skies.
2. The variation between the maximum value (Mx) and the P95 was small and increased slightly in the central hours of the day. So, the maximum values cannot be regarded as representative of the UV irradiance in the study area.
3. The variation between the mean (M) and median (Md) was small and variable during the day, although the median was larger than the mean in the afternoon.
4. The absolute maximum values of the irradiance were: 11200 W/cm^2 (UV (A+B)) and 103 W/cm^2 (UV (C)) and corresponded in all cases to 12:00 LST.
5. Standard deviation values were low compared to the mean, although they decreased towards midday when radiation was higher. Towards the end of the day, the SD values then increased.
6. The variation of the irradiation values can be analysed using the CV index. Based on the results, the CV values ranged from: 1.8 to 21.2% for UV (A+B); 1 and 25.5% for UV(C) irradiance. The small scatter found at both irradiances shows the acceptable accuracy of the instruments used for the measurement.

3.2. Linear regression of UV versus geographical latitude, longitude, and altitude

Changes in the intensity of UV radiation have been linked to changes in latitude, longitude, and altitude. Latitude, longitude, and elevation trends from surface UV measurements are also presented (Figures 3, 4). In general, the UV values increase with decreasing length. The intensity of UV radiation, as shown in Figure 3a, is related to longitude (r^2= 0.15 for UV (A+B); r^2= 0.13 for UV (C)). The UV intensity varies with local latitude (Figure 3b).

The scatter plot between altitude and UV radiation shows a consistent linear pattern (Figure 4a). With decreasing altitude, UV has a downward trend. The UV variation of different points with the same height is due to the fact that these points have different surface properties. In this study, some spread between UV radiation and altitude was observed, mainly for UV values (A+B) between 6000-10000 W/cm^2 and UV-C between 50-100 W/cm^2 (Figure 4a). To further investigate the relationship between UV and altitude, mean UV values were calculated at each altitude level. Figure 4b shows the relationship between mean UV and each altitude level. A strong linear relationship is observed between mean UV (C) and altitude with a regression coefficient value of 0.84. While the coefficient value of 0.04 was observed for the relationship between mean UV (A+B) and altitude. Figure 4b shows increases in UV irradiance per 50 meter height from 5000 W/cm^2 in UV (A+B), 42 W/cm^2 in UV (C). The measured UV irradiance increased with altitude. This is because there are fewer atmospheres at high altitudes and therefore less scattering and absorption takes place. In addition, tropospheric ozone is mainly found at low altitudes, as are other pollutants such as aerosols. At high altitudes there are also typically fewer clouds, or even clouds underneath, which act as a reflective surface with a high albedo, increasing UV irradiance compared to less elevated locations (Lindfors et al., 2018).

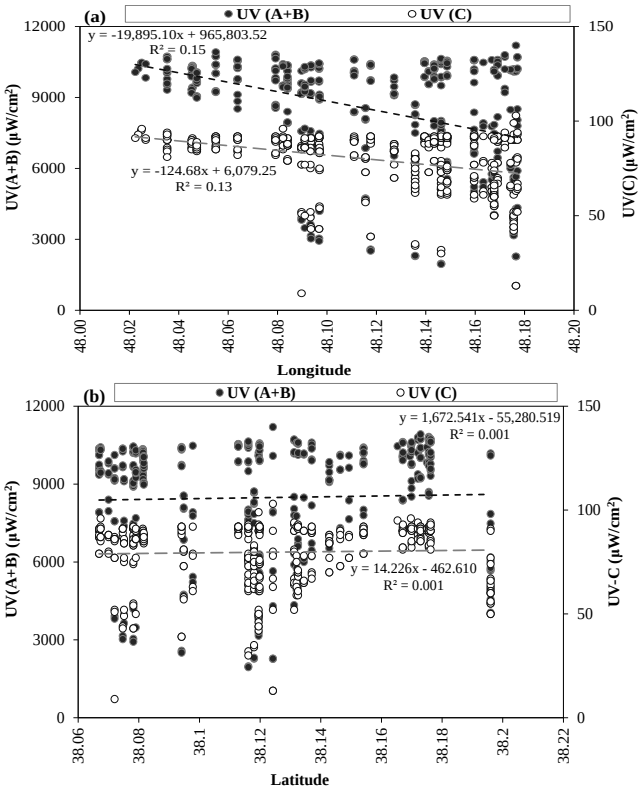

Figure 3. Scatter plot of UV (A+B) and UV (C) solar irradiances vs. local longitude (a) and local latitude (b).

3.3. Patterns of UV radiation in different land cover types

Different kinds of reflective surfaces produce different effects on UV radiation. The distributions of UV (A+B) and UV (C) solar irradiances were examined across different land cover types (Figure 5). The mean UV (A+B) among different land cover types is as follows (in descending order): water (8861), soil (8857), asphalt (8739), concrete (8384), cultivated areas (8494), and grass (7841) (Figure 5a). The mean UV (C) among different land cover types in descending order is as follows: water (83), soil (83), asphalt (82), cultivated areas (80), concrete (79), and grass (75) (Figure 5b). All the values are in the unit of µW/cm^2.

This contribution has been peer-reviewed. The double-blind peer-review was conducted on the basis of the full paper.
https://doi.org/10.5194/isprs-annals-X-4-W1-2022-327-2023 | © Author(s) 2023. CC BY 4.0 License.

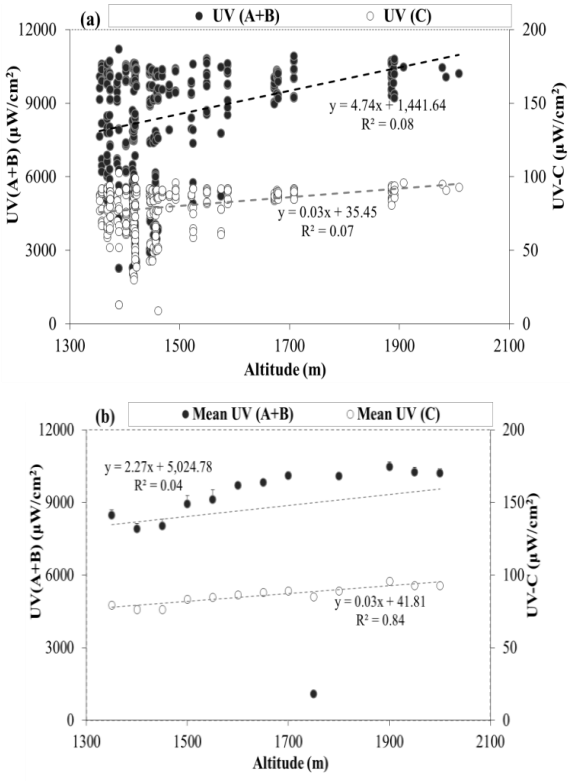

Figure 4. Scatter plot of UV (A+B) and UV (C) solar irradiances vs. altitude (a), and trend line of mean values of UV (A+B) and UV (C) solar irradiances vs. altitude (b).

Different surfaces are examined for fluctuations in the reflection intensity of UV (A+B) and UV (C) solar radiation with daily time differences (Figure 6). The trend towards the variety of all artificial and natural surfaces is about the same. The trend is slightly different for water, which cannot be explained because of the small number of samples. The results of the reflectance analysis for six different surfaces showed that the maximum UV (A+B) and UV (C) solar radiation occurs between 11 and 13 hours (Figure 6).

Fluctuations in UV (A+B) and UV (C) solar radiation versus diurnal time differences of all artificial and natural surfaces are approximately the same. However, mean UV radiation varies depending on land cover type. Water and land cover types are the most vulnerable areas with the highest UV exposure. The result is consistent with some previous studies that suggested that water along with snow and sand has high reflectivity for solar UV radiation (Chadyšiene and Girgždys, 2008; Diffey, 2018). The water land cover type in this study area is open water bodies, which have minimal protection from UV radiation and high UV radiation exposure, making their UV radiation higher than that of the others. Water absorbs most of the solar radiation, resulting in significant warming and increased penetration of UV radiation into the open water (Häder et al. 2015). In general, soft surfaces such as grass and built-up areas reflect less UV radiation than hard surfaces such as concrete in the study area. Similar results were obtained from Liu et al. (2014) and Turner and Parisi (2018) in the previous studies. Cultivated areas have higher UV values than grasses. Typically impervious materials (asphalt and concrete) have higher levels of UV radiation. It is necessary to mention that due to sunlight angle limitations; Shadows from tall buildings on asphalt along roads can greatly reduce the total amount of UV solar radiation reaching the ground surface, resulting in low UV radiation in the study area. On average, the highest UV values were from the natural cover, i.e. water and soil, obtained with almost the same values of 8860 and 83 W/cm^2 for UV (A+B) and UV (C) respectively, while the lowest UV values were obtained by grass of 7840 and 75 W/cm^2 for UV (A+B) or UV (C).

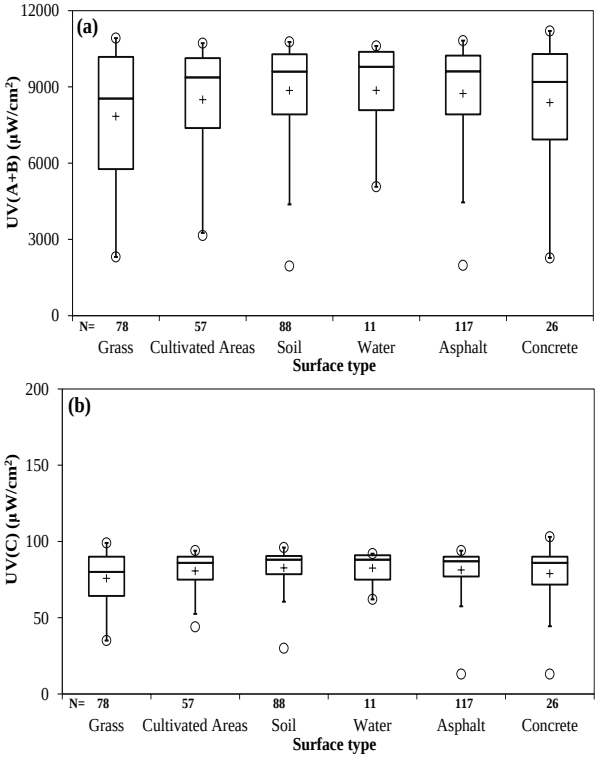

Figure 5. Distribution of UV (A+B) (a) and UV (C) (b) solar irradiances across different land cover types (the upper and lower bounds of the box plots indicate the Q3-Q2 and Q2-Q1 quartiles of the values, the whiskers represent the Q3- extreme outlier and extreme outlier -Q1 quartiles, the cross represents the mean, the midlines represent median, and the top and bottom ellipses illustrate the maximum and minimum values, respectively). N is the number of observations for each land cover type.

4. CONCLUSIONS

This study examined for the first time the hourly trend of UV radiation in Iran from measurements in June 2019 and focused only on clear sky conditions. Measured data at 5 minute intervals was used to generate the most representative statistical properties of both hourly UV (A+B) and UV (C) irradiance values. In addition, the effects of some environmental factors such as time of day and geographic location, as well as surface type, on UV radiation were examined. UV radiation varies depending on the time of day and year, because the higher the sun is in the sky, the higher the UV radiation. The results of the present study are consistent with the rationale. Solar UVR is strongest at solar noon (the point halfway between sunrise and sunset) when the sun is highest in the sky. With regard to the hourly values, the analysis shows that the minimum values can be regarded as representative of the UV properties in the study area. The UV (A+B) and UV (C) irradiance was 11200 and 103

W/cm^2 respectively at solar noon. Geographically, UV is strongest at the equator; at higher latitudes, the sun is lower in the sky, resulting in lower UV levels. UV intensity increases with altitude. In addition, UV radiation can reflect off many surfaces, including grass, asphalt, sand and water. The amount of reflected UV can be as high as 90% or as low as 1%, depending on the surface (Young, 2009).

Continuous measurements of UV radiation are of great importance to analyse their spatial and temporal distribution in different atmospheric conditions. Unfortunately, the high cost of instrumentation makes this type of measurement almost impossible in Iran, as well as in other countries (Foyo-Moreno et al., 1999; Porfirio et al., 2012). An alternative to analysing UV radiation is therefore to use physical or empirical models, especially the empirical models that relate UV radiation to different parameters of solar radiation (Escobedo et al., 2009), and are widely used because they need relatively less data. The variation trend of UV radiation in the study area can provide the scientific basis for an understanding of the interaction between the radiant energy of the sun and the geographic location of the Earth, which will play a fundamental role in many areas such as ecological processes, atmospheric environment, energy budget, and human health. In the meantime, the empirical models for the analysis of UV radiation will be considered in future studies in the study area.

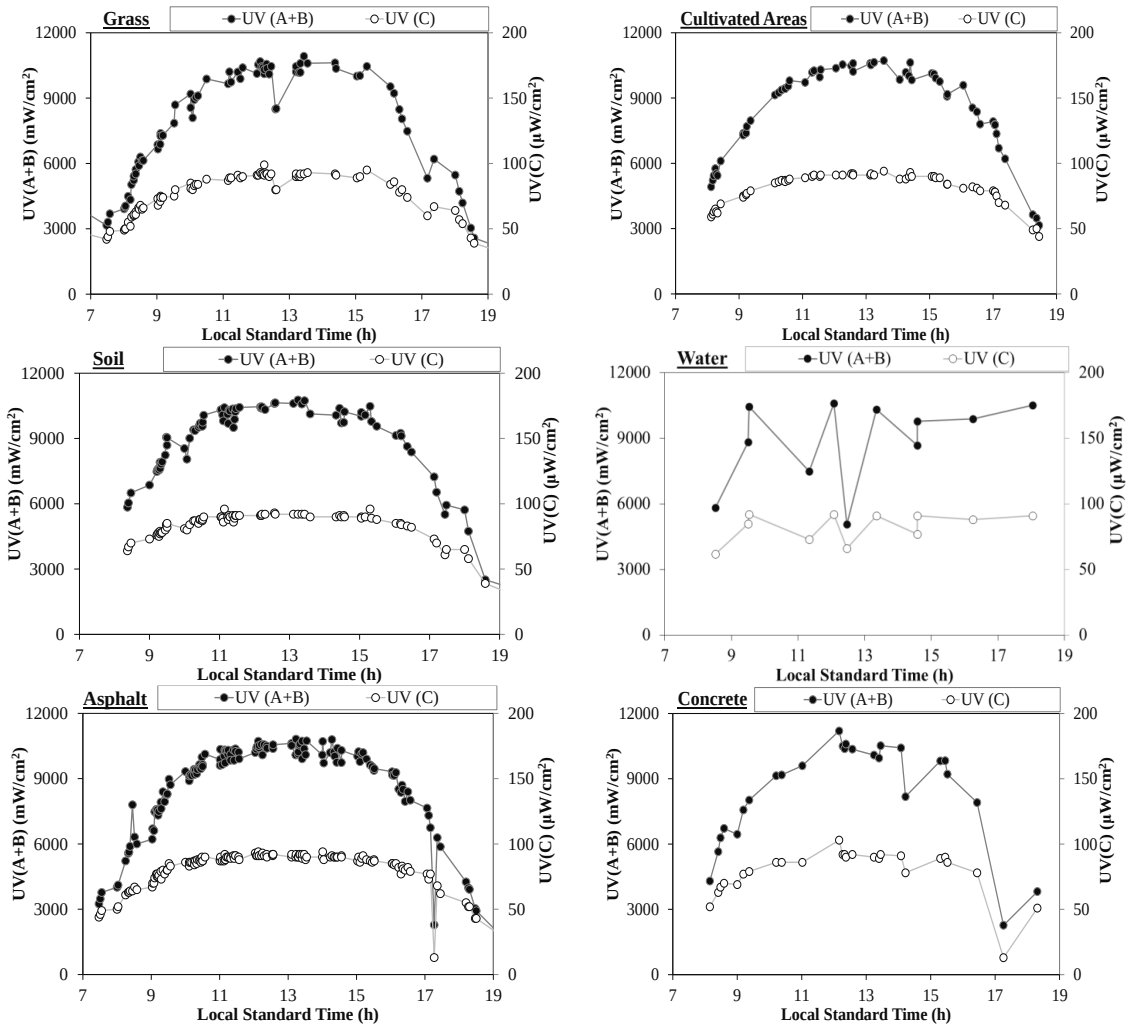

Figure 6. Daily patterns of UV (A+B) and UV (C) solar irradiances across different land cover types (a), under clear sky conditions: for the period (June 2019).

REFERENCES

Akhlaghi, M., Radfard, M., Arfaeinia, H., Soleimani, M., Fallahi, A., 2018. Ultraviolet radiation rate in Mashhad, Iran. Data in Brief, 19, 1086–1091.

Babaee, S.A.R., Pourarjomand, B., Ahmadzadeh, A., 2016. Measurement of solar ultraviolet radiation intensity type A and B in Qazvin (2013-14). *JQUMS*, 20 (3), 33-39.

Balasaraswathy, P., Kumar, U., Srinivas C.R., Nair, S., 2002. UVA and UVB in sunlight, Optimal Utilization of UV rays in Sunlight for phototherapy. *Indian J Dermatol Venereol Leprol*, 68, 198-201.

Bilbao, J., Miguel, D., Miguel, A., 2011. Analysis and cloudiness influence on UV total irradiation. *Int J Climatol*, 31, 451-60.

Bouzarjomehri, F., Tsapaki, V., 2012. Measurement of solar ultraviolet radiation in Yazd, Iran. *Int J Radiat Res*, 10 (3 and 4), 187-191.

Chadyšiene, R., Girgždys, A., 2008. Ultraviolet radiation albedo of natural surfaces. *J. Environ. Eng. Landsc. Manag*.16, 83–88.

Diffey, B.L., 2018. Time and Place as Modifiers of Personal UV Exposure. *Int. J. Environ. Res. Public Health*, 15, 1112.

Escobedo, J.F., Gomes, E.N., Oliveira, A.P., Soares, J., 2009. Modeling hourly and daily fractions of UV, PAR and NIR to global solar radiation under various sky conditions at Botucatu, Brazil. *Applied Energy*, 86, 299-309.

Foyo-Moreno, I., Vida, J., Alados-Arboledas, L., 1999. A simple all weather model to estimate ultraviolet solar radiation (290-385 nm). *Journal of Applied Meteorology*, 38, 1020-6.

Häder, D.P., Williamson, C.E., Wängberg, S.Å., Rautio, M., Rose, K.C., Gao, K., Helbling, E.W., Sinha, R.P., Worrest, R., 2015. Effects of UV radiation on aquatic ecosystems and interactions with other environmental factors. *Photochem. Photobiol. Sci.*, 14, 108-126.

Hooshyar, L., Barugh, H., 2014. The Role of Tourism in Sustainable Urban Development (Random Sample: Sarein). *J Art Arch Stud*. 3 (2), 95-101.

Kadad, I.M., Ramadan, A.A., Kandil, K.M., Ghoneim, A.A., 2022. Relationship between Ultraviolet-B Radiation and Broadband Solar Radiation under All Sky Conditions in Kuwait Hot Climate. *Energies*, 15, 3130. https://doi.org/10.3390/en15093130

Khodadost, M., Yavari, P., Khodadost, B., Babaei, M., Sarvi, F., Khatibi, S.R., Barzegari, S., 2016. Estimating the Esophagus Cancer Incidence Rate in Ardabil, Iran: A Capture-Recapture Method. *Iran J Cancer Preven*, 9 (1), e3972.

Kolahdoozan, S., Sadjadi, A., Radmard, A.R., Khademi, H., 2010. Five common cancers in Iran. *Arch Iran Med*. 13(2), 143–6.

Lindfors, A.V., Kujanpää, J., Kalakoski, N., Heikkilä, A., Lakkala, K., Mielonen, T., Sneep, M., Krotkov, N.A., Arola, A., Tamminen, J., 2018. The TROPOMI surface UV algorithm. *Atmos. Meas. Tech*., 11, 997–1008.

Liu, C., Wang, F., Gao, Y., Yang, Z., Hu, L., Gao, Q., Ri, J., Liu, Y., 2014. The Enhancement of Biological Occular UV Radiation on Beaches Compared to the Radiation on Grass. *J. Photochem. Photobiol. B Boil*. 141, 106–112.

Madronich, S., Tilmes, S., Kravitz, B., MacMartin, D.G., Richter, J.H., 2018. Response of Surface Ultraviolet and Visible Radiation to Stratospheric SO2 Injections. *Atmosphere*, 9, 432. doi: 10.3390/atmos9110432.

Martinez-Lozano, J.A., Tena, F., Utrillas, M.P. 1996. Measurement and analysis of ultraviolet solar irradiation in Valencia, Spain. *International Journal of Climatology*, 16, 947-955.

Pashiardis, S., Kalogirou, S.A., Pelengaris, A., 2017. Statistical Analysis and Inter- Comparison of Solar UVA and Global Radiation for Athalassa and Larnaca, Cyprus. *SM J Biometrics Biostat*. 2(4), 1020.

Porfirio, A.C.S., De Souza, J.L., Lyra, G.B., Lemes, M.A.M., 2012. An assessment of the global UV solar radiation under various sky conditions in Maceió-Northeastern Brazil. *Energy*, 44, 584-592.

Shahbazi-Gahrouei, D., Setayandeh, S., Gholami, M. 2013. A review on comparison of natural radiation in Iran with other countries. *Int. J. Low Radiation*, 9 (1), 1–11.

Tavoosi, T., Delara, G., 2010. Climatic zoning of Ardabil Province. Scientific and technical journal of Nivar, N. 70-71. P.47-52 (in Persian).

Thomas, P., Swaminathan, A., Lucas, R., 2012. Climate change and health with an emphasis on interactions with ultraviolet radiation: a review. *Glob Change Biol*, 18, 2392-405.

Turner, J., Parisi, A.V., 2018. Ultraviolet Radiation Albedo and Reflectance inReview: The Influence to Ultraviolet Exposure in Occupational Settings. Int. J. Environ. Res. *Public Health*, 15, 1507.

Vatani, J., Raei, M., Asadi, M., 2013. Assessing the ultraviolet exposure level in welding workers of Sar-Cheshmeh copper complex. *Zahedan Journal of Research in Medical Sciences*, 15(4), 76-7.

Wald, L., 2018. Basics in solar radiation at Earth surface. (hal-01676634)

Wild, M., Gilgen, H., Roesch, A., Ohmura, A., Long, C.N., 2005. From dimming to brightening: decadal changes in solar radiation at Earth's surface. *Science*, 308, 847-9.

Young, C., 2009. Solar ultraviolet radiation and skin cancer. *Occupational Medicine*, 59 (2), 82–88.